# Mechanical Spectroscopy Studies on a Side-Chain Liquid Crystalline Polysiloxane. Comparison with Dielectric and DSC Data

**J. F. Mano*,†,‡ and J. L. Gómez Ribelles§**

*Department of Polymer Engineering, University of Minho, Campus de Azurém, 4800-058 Guimarães, Portugal; 3B's Research Group—Biomaterials, Biodegradables and Biomimetics, Department of Polymer Engineering, University of Minho, Campus de Gualtar, 4710-057 Braga, Portugal; and Center for Biomaterials and Department of Applied Thermodynamics, Universidad Politécnica de Valencia, P.O. Box 22012, E-46071 Valencia, Spain*

*Received May 23, 2002*

ABSTRACT: The viscoelastic properties are investigated for a side-chain liquid crystalline polymer using dynamic mechanical analysis (DMA) in the temperature region comprising the glass transition and the smectic phase. Two main relaxation processes are found, labeled α and $\delta$ relaxations, with increasing temperature. The results are compared with dielectric relaxation spectroscopy (DRS) and differential scanning calorimetry (DSC) results previously reported. The α-relaxation is well described by the KWW and Havriliak−Negami models, featuring a broad distribution of relaxation times, which depend on temperature according to the VFT model above $T_g$. The mechanical, dielectric, and calorimetric results in the region of the α-relaxation show similar behavior, indicating that this process should be assigned to the segmental mobility of the main chain. This hypothesis could be consistent with the onset of faster modes within the mesogens, mainly involving their transverse dipole component, for the case of the dielectric response of the α-relaxation. The $\delta$-relaxation detected by both DMA and DRS has a similar origin, exhibiting a nearly Debye behavior. This process involves the motions of the bulky mesogenic groups and is not visible by DSC, as the increase of entropy during its occurrence is not significant.

## I. Introduction

The typical structure of side-chain liquid crystalline polymer (SCLCPs) consists of a flexible polymeric backbone with mesogenic groups attached laterally to it via a flexible spacer, usually consisting of an alkyl chain $-(CH_2)_x-$.[1,2] This spacer allows to decouple and enhance, to some extent, the mobility of the mesogen from that of the main chain. These polymers may thus present liquid crystalline properties, generally between the glass transition ($T_g$) and the clearing temperatures ($T_c$).

There is a clear interest, for both fundamental and applied research groups, in the investigation of such materials. The hybrid nature of SCLCPs confers to them the most general physical (density, heat capacity, etc.), mechanical and rheological properties of polymers, and, simultaneously, the anisotropic and peculiar optical features of low molecular weight liquid crystals, albeit on a much slower response time scale. This combination of properties makes SCLCPs attractive for a variety of commercial applications, including optical data storage, nonlinear optics, holographic applications, stress sensors, and chromatography.[1]

The molecular mobility in SCLCPs is complex, giving rise, for example, to relaxation processes that are not observed in conventional polymers, such as the $\delta$-relaxation, which will be discussed in the text. SCLCPs have also the particular ability to maintain the liquid crystalline order into the glassy state. This new class of glassy structures may be very interesting to make new physics related with the elucidation of the dynamics of the glass transition in glass-forming systems, which have not been fully understood.[3,4] In conventional amorphous polymer systems the kinetics of these molecular motions are described phenomenologically by a broad distribution of characteristic times due to the different environment felt by the constrained inter- and intramolecular segmental motions of the polymer backbone. In SCLCPs, because of the long spacers attached to the polymer backbone, such motions also occur in different environments in which the local concentration of the methylene chains fluctuates, increasing the complexity of the motions involved in the glass transition.[5]

The molecular mobility in SCLCPs has been investigated by a variety of techniques, but mainly by dielectric spectroscopy (DRS) (see references along this text and ref 6). DRS is an attractive technique due to the broad range of frequencies available (up to 16 decades). Particularly for the SCLCPs, this technique enables the study, for example, of the $\delta$-relaxation in different phases, such as the isotropic liquid and the liquid crystalline phase. The dynamic mechanical analysis (DMA) is the mechanical spectroscopy technique analogue to DRS. This technique has not been often used in the glassy and liquid crystalline phases of SCLCPs, despite most of these materials being in such states at ambient temperature.

Therefore, DMA could allow for the understanding of the solid-state rheological properties at operative temperatures of such materials and can also provide complementary information on the dynamics of the relaxation processes that occur in those temperature regions. Some rheological studies on SCLCPs have been carried out at temperatures well above $T_g$, which may be important for optimizing their processing, including,

† University of Minho, Campus de Azurém.
‡ University of Minho, Campus de Gualtar.
§ Universidad Politécnica de Valencia.
* Author for correspondence: e-mail jmano@dep.uminho.pt.

10.1021/ma020800p CCC: $25.00 
Published on Web 03/26/2003

for example, the understanding of the influence of flow history on the general structure (including the molecular alignment), mainly when the material goes from the isotropic to the anisotropic state.[7−10] However, to the best of our knowledge, only two works have been devoted to DMA studies below the clearing temperature, including the glassy state, although the $\delta$-relaxation was not investigated in detail.[11,12] Among these works, a side-chain liquid crystalline polysiloxane copolymer was investigated by Etienne et al.,[12] having a short spacer length of $-(CH_2)_3-$. In the present work we investigate a polymer with the same backbone but with a longer spacer, in both glassy and liquid crystalline phases.

As will be discussed in the next section, the assignment at the molecular level of the relaxations observed by DRS in the glassy and liquid crystalline phases is still controversial. This work also pretends to give a further contribution to that issue due to the fact that DMA probes the reorientation dynamics in a different way of the dielectric techniques. In DRS, the more or less constrained mobility of the dipole moments is monitored. As SCLCPs usually bear a considerable dipole moment (at least in the side groups), the molecular mobility of the material may be probed in the different structural regions. DMA may be seen as a complementary technique that has the advantage to directly measure the different molecular motions within the entire polymer structure, even if they occur in nonpolar regions.

## II. Assigment of Relaxation Processes in Side-Chain Liquid Crystalline Polymers

At low temperatures, well below $T_g$, SCLCPs exhibit relaxations associated with local mobility within the side groups, often labeled as $\beta$ and $\gamma$, with decreasing temperature. Several features of these thermally activated processes, such as activation energies, temperature location, and distribution of characteristic times, are similar to those observed in conventional amorphous polymers.[13−16]

Above $T_g$ essentially two relevant relaxation processes are observed by DRS, labeled $\alpha$ and $\delta$, with increasing temperature. The work of Williams and co-workers studied SCLCPs in different alignment states (a list of references can be found in refs 17 and 18), namely, those where the liquid crystalline director of the mesogens, **n**, is aligned parallel (homeotropic) or perpendicular (planar) to the direction of the applied ac filed. The dielectric behavior measured in the homeotropic state is dominated by the motions of $\mu_l$ (longitudinal component of the mesogen's dipolar moment, $\mu$), the transverse motions being ineffective. On the other hand, with the planar alignment the motions of the transverse component of $\mu$, $\mu_t$, will be much more favorable. More specifically, it was found that the deconvolution of the dielectric spectra for homeotropic or planar fully aligned samples produces four fundamental modes of motions. The combination of dipole relaxation modes 00 and 10 involves the motions of $\mu_l$, and the modes 01 and 11 involves $\mu_t$. For partially aligned samples the complex permittivity, $\epsilon^*(\omega) = \epsilon'(\omega) - i\epsilon''(\omega)$, is given, approximately, by the relation[19]

$$\epsilon^*(\omega) = (1 + 2S_d)\epsilon^*_{||}(\omega)/3 + 2(1 - S_d)\epsilon^*_{\perp}(\omega)/3 \quad (1)$$

where $S_d$ is the macroscopic director order parameter, which describes the average orientation of the local directors **n** with respect to the measuring field direction, and $\epsilon_{||}$ and $\epsilon_{\perp}$ are related to $\mu_l$ and $\mu_t$, respectively, according to

$$\epsilon^*_{||}(\omega) = \epsilon_{\infty||} + \frac{G}{3kT}[(1 + 2S)\mu_l^2 F^l_{||}(\omega) + (1 - S)\mu_t^2 F^t_{||}(\omega)] \quad (2a)$$

$$\epsilon^*_{\perp}(\omega) = \epsilon_{\infty\perp} + \frac{G}{3kT}[(1 - S)\mu_l^2 F^l_{\perp}(\omega) + (1 + S/2)\mu_t^2 F^t_{\perp}(\omega)] \quad (2b)$$

where $\epsilon_{\infty||}$ and $\epsilon_{\infty\perp}$ are limiting high-frequency permittivities, $G$ is a constant, $S$ is the local order parameter for the mesophase, and the $F^i_j(\omega)$ are given by the one-side Fourier transform ($F$) of time-correlation functions for the angular motions of $\mu_l$ and $\mu_t$: $F^i_j(\omega) = 1 - i\omega F[F^i_j(t)]$.

According to this theory, it was proposed that the $\delta$-relaxation should be assigned to the $F^l_{||}(\omega)$ process (00 mode), i.e., to the motions of the mesogens along their short axis. This process enhances with progressive homeotropic alignment ($S_d = 1$) and can be removed in a planar aligned sample, $S_d = -1/2$.[17] The three remaining faster modes should comprise the broader $\alpha$ process observed experimentally. Therefore, the $\delta$-relaxation would involve motions of $\mu_l$ and the $\alpha$ process contains contributions from both $\mu_l$ and $\mu_t$. These assignments proposed by the work of Williams and co-workers were also exploited by many other authors.[6,20−26] Some authors emphasized the fact that the $\alpha$-relaxation in SCLCPs should be mainly due to the motions of $\mu_t$, i.e., to the rotation of the mesogenic units along their long axis.[22]

The attribution of the $\delta$-relaxation at the molecular level is consensual in the literature. However, the assignment of the $\alpha$-relaxation as observed by DRS has been controversial. In fact, other investigators interpreted this process to the cooperative segmental motions within the polymer backbone, as detected in amorphous or semicrystalline conventional polymers, associated with the dynamic glass transition.[13−15,27,28] There are some arguments that support this attribution. The temperature dependence of the $\alpha$-relaxation rate shows a curvature in an Arrhenius plot that can be fitted by a Voguel−Fulcher−Tamman (VFT) equation, which is characteristic for glass-forming systems. Moreover, at low frequencies the temperature of maximum loss of this process seems to be compatible to the calorimetric glass transition.[13,28] In a more detailed study, it was found that the dynamics of the glass transition studied by enthalpy relaxation, as computed with phenomenological models from differential scanning calorimetry data (DSC), agrees with the dielectric results.[29] The same study also permitted to conclude that the form parameter of the relaxation time distribution is similar for the calorimetric glass transition and for the dielectric $\alpha$-relaxation. Therefore, the attribution of the $\alpha$-relaxation to a pure dipolar activated process within the side groups should be questioned. Temperature-modulated DSC was also used to demonstrate that the dynamic glass transition of a liquid crystalline polymethacrylate follows the same kinetics as the dielectric $\alpha$-relaxation.[30]

The comparison of DRS results with calorimetric ones are interesting because the former technique is sensitive

to dipole fluctuations while the latter responds to entropy fluctuations. Dynamic mechanical analysis (DMA) provides another source of a structural probe due to its sensitivity for the different stress/strain environments. In the present work DMA will be used in this context to provide further indications about the origin of the α-relaxation found by DRS in SCLCPs.

## III. Experimental Section

**A. Materials.** The liquid crystalline polymer studied in this work is from Merck (catalog no. LCP1) and has the following structure:

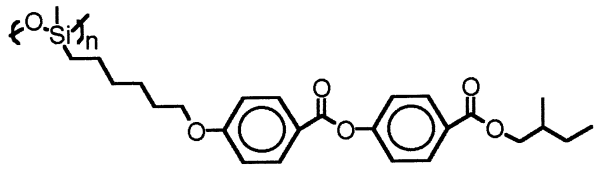

with $n \sim 40$. According to the manufacturer, it has a glass transition temperature near −7 °C and a smectic C/isotropic transition at 76.8 °C.

**B. Apparatus.** Differential scanning calorimetry (DSC) experiments were carried out in a Perkin-Elmer DSC7 differential scanning calorimeter with controlled cooling accessory. All the experiments were performed on a sample weighing 10.293 mg at a heating rate of 10 K/min, from −30 to 45 °C. More details about the experimental setup may be found elsewhere.[29]

The dynamic mechanical measurements were carried out using a DMA7e Perkin-Elmer apparatus with controlled cooling accessory in the temperature range from −30 to +60 °C. High-purity helium was used to improve heat transfer to the sample environment during the experiments. Isochronal experiments at $f = 1$ Hz were carried out at 2 K min$^{-1}$ in both flexural and compression mechanical configurations. Flexural experiments were conducted in a three-point bending mode, where the sample, shaped in a cylindrical geometry with ∼1.5 mm diameter, was placed in a 5 mm bending platform. Such experiments were conducted in the region around $T_g$ (between −30 and 20 °C). In the higher temperature region compression experiments were carried out, using parallel plates of 5 mm diameter. In both isochronal experiments, a static stress of $5.4 \times 10^4$ Pa and a dynamic stress with $4.5 \times 10^4$ Pa amplitude were imposed to the sample.

Also, isothermal experiments were performed in the flexural mode, between −20 and 5 °C. The frequency range used was 0.6−30 Hz.

The temperature calibration was performed with distilled water and using the apparatus in the static mode. In compression experiments a drop of water was placed between the plates. A small force of 10 mN was imposed to the ice by the top plate, and the position of it was monitored during an heating experiment, enabling to clearly identify the melting of the ice. For the flexural test a drop of distilled water was located in the top center of a small plastic piece, which was placed over the bending platform. The probe tip imposed a small force over the ice, and again, the rapid displacement during a heating experiment allowed to detect the melting of the ice. The temperature read by the sensor at the occurrence of the melting enable to correct the temperature in the studied temperature region. Calibration experiments at 2 K min$^{-1}$ allowed to calibrate the isochronal experiments. Calibration experiments using the flexural mode performed at different heating rates were used to correct the temperature reading of the isothermal experiments by extrapolating the read melting temperatures of ice to zero heating rate.

## IV. Results and Discussion

**A. DSC Results.** Figure 1 shows two DSC traces of LCP1 obtained during heating after different previous thermal histories. The quenched sample presents a typical step in the thermogram around $T_g$ (solid line). The sample previously cooled at 1 K min$^{-1}$ from the equilibrium shows the endothermic peak corresponding to the occurrence of structural relaxation (dashed line in Figure 1). This phenomenon occurs in glass-forming systems when the supercooled liquid undergoes an approach to the equilibrium in the glassy state. The area of this peak with respect to the first trace is related to the enthalpy recovered during the slow cooling rate. The DSC results clearly confirm that the calorimetric glass transition of LCP1 occurs at −9 °C, as measured by the midpoint of the rise of $c_p$ in the transition, for a heating rate of 10 K min$^{-1}$ and after a quenching program from equilibrium.

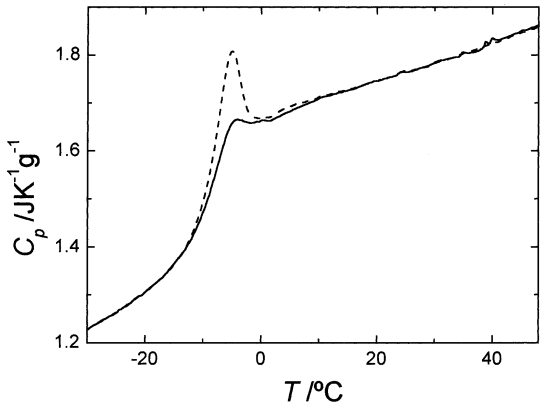


**Figure 1.** DSC scans on LCP1 at 10 °C/min after quenching (solid line) and after cooled at 1 °C/min from the equilibrium (dashed line).

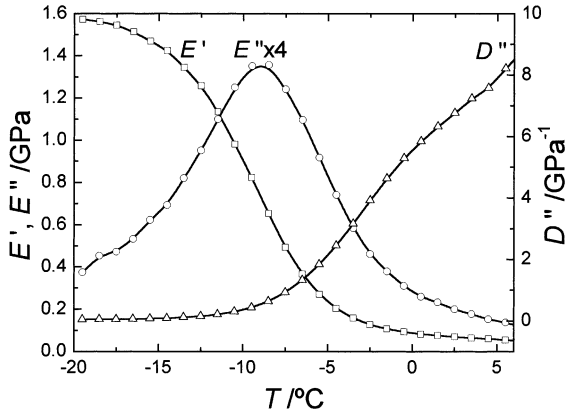


**Figure 2.** Isochronal mechanical spectroscopy scans at 1 Hz on LCP1 using the flexural mode. The rough data were smoothed by averaging the values through intervals of 1 °C.

**B. Rheological and Dielectric Results in the Region of the α-Relaxation.** *1. Results in the Frequency Domain*. Flexural isochronal experiments were carried out at a frequency of $f = \omega/2\pi = 1$ Hz in the region of the glass transition of LCP1. The storage and loss moduli ($E'$ and $E''$) and the loss compliance ($D''$) are shown as a function of temperature in Figure 2. A relaxation process was observed with a temperature of maximum of $E''$ that is in the region of the calorimetric glass transition. The loss compliance peak is not clearly resolved due to the existence of a second higher temperature process, which will be studied later. Therefore, we opted to investigate in more detail this relaxation in terms of the mechanical modulus.

Isothermal experiments were performed in this temperature region. A master curve for the loss modulus

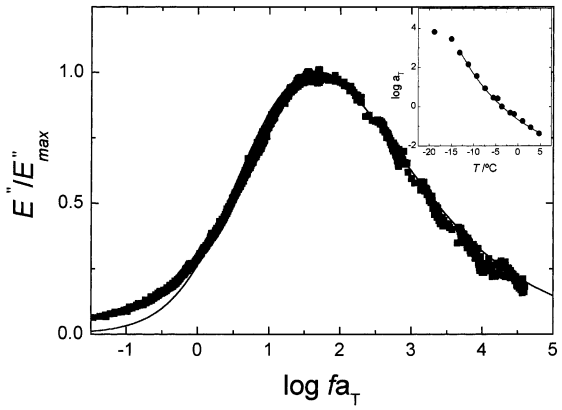


**Figure 3.** Master curve for normalized $E''$ in the region of the glass transition of LCP1 at a reduced temperature of −3.6 °C. The solid line corresponds to the best fit with the KWW model. The inset graphics show the temperature dependence of the horizontal shift factors and the corresponding fit of the data above $T_g$ with the WLF equation (solid line).

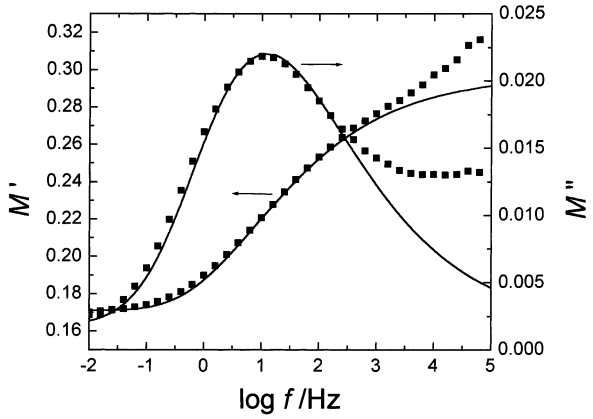


**Figure 4.** Real and imaginary components of the dielectric modulus at −5 °C. The solid lines correspond to the fit of the experimental data according to the KWW model. The high-frequency points were skipped in the fitting because they are affected by the $\beta$-relaxation.

was constructed by shifting along the logarithm of the frequency axis the isothermal data, according to the time−temperature superposition principle.[31] Figure 3 display the generated normalized master curve for $E''$ reduced at a reference temperature of $T_{ref} = -3.6$ °C as a function of reduced frequency $fa_T$. The corresponding shift factors, log $a_T$, are plotted against temperature in the inset graphics of Figure 3. This plot shows a curved trend above −15 °C that can be modeled with the VFT or WLF equations (solid line for the WLF fit). However, in the low-temperature side a clear deviation of this tendency is observed. This corresponds to the change from the liquid behavior to the nonequilibrium glass dynamics, described by an Arrhenius equation, that is usually observed in glass-forming materials (see, for example, the discussion of this phenomenon in ref 32). This is also a good indication that the observed mechanical process is similar to the α-relaxation observed in amorphous systems corresponding to the segmental motions within the polymer backbone.

The dielectric permittivity, $\epsilon^* = \epsilon' - i\epsilon''$, is given by the one-sided Fourier or pure imaginary Laplace transform of the time derivative of the normalized response function, $\Phi(t)$, for the dielectric polarization of the system.[33] One can use this formalism for the mechanical response that, in terms of the complex mechanical modulus, $E^*(\omega) = E'(\omega) + iE''(\omega)$, reads

$$\frac{E^*(\omega) - E_U}{E_R - E_U} = \int_0^\infty \left[-\frac{d\Phi(t)}{dt}\right] \exp(-i\omega t)\, dt \qquad (3)$$

where U and R designate unrelaxed and relaxed moduli values, respectively, and $i^2 = -1$. On the other hand, the α-relaxation in amorphous or semicrystalline systems is properly described by the Kohlrausch−Williams−Watts (KWW),[34,35] or stretched exponential, correlation function

$$\Phi(t) = \exp\left[-\left(\frac{t}{\tau_{KWW}}\right)^{\beta_{KWW}}\right] \qquad (4)$$

where $\tau_{KWW}$ is a characteristic time and $\beta_{KWW}$ ($0 < \beta_{KWW} \leq 1$) is a parameter that describes the nonexponential behavior of the correlation function. The master curve for the loss modulus in Figure 3 was fitted with eqs 3 and 4 (solid line in Figure 3). The optimized parameters were $\beta_{KWW} = 0.37$ and $\tau_{KWW} = 0.002\,4$ s. The KWW relaxation time is related to the frequency of maximum loss modulus, $\omega_{max}$, at the same temperature, by[36] $\log(\omega_{max}\tau_{KWW}) = -0.263(1 - \beta_{KWW})$. Therefore, at −3.6 °C, we have $f_{max} = \omega_{max}/2\pi = 45.1$ Hz for $E''$.

The comparison between rheological and dielectric results must be made carefully, and it is still an open problem. However, if we are investigating the mechanical modulus, the corresponding dielectric analogue to work with is the dielectric modulus: $M^*(\omega) = 1/\epsilon^*(\omega) = M'(\omega) + iM''(\omega)$.

By using $M^*$, the dynamics of the relaxational processes are described in terms of relaxation times instead of retardation times, which are obtained from the frequency of maximum of loss permittivity.

Figure 4 shows the real and imaginary components of the dielectric modulus as a function of frequency for the studied polymer at −5 °C. The curve was obtained from permittivity data obtained in the laboratory of Prof. G. Williams (University College of Swansea, UK) and reported elsewhere.[37] The dielectric α-relaxation is clearly detected in this frequency window. At higher frequencies, the $\beta$-relaxation starts to overlap with the former process.[37] An attempt was made to fit the lower frequency side of both $M'(\omega)$ and $M''(\omega)$ using the KWW model (eqs 3 and 4). The adjusted curves (solid lines in Figure 4) describe well the results in the low-frequency side. In this case we found $\beta_{KWW} = 0.32$. Moreover, the KWW parameter obtained from DSC results yield 0.35.[29] The values of $\beta_{KWW}$ found for amorphous systems ranges usually between 0.3 and 0.5.[38] Therefore, the results obtained from the different techniques in LCP1 point to a broad distribution of characteristic times for the α relaxation.

*2. Arrhenius Diagram.* Both real and imaginary components of the dielectric moduli are shown against frequency in Figure 5 for temperatures between −10 and 10 °C. It is clear the increasing of influence of the $\beta$-relaxation in the high-frequency axis as temperature increases. To determine with more precision the position of the α-relaxation of LCP1, the dielectric modulus was fitted according to a sum in the frequency axis of two independent dielectric responses, each of them described by a Havriliak−Negami (HN) model function. The HN expression for the complex dielectric modulus of each relaxation process may be obtained from the transpor-

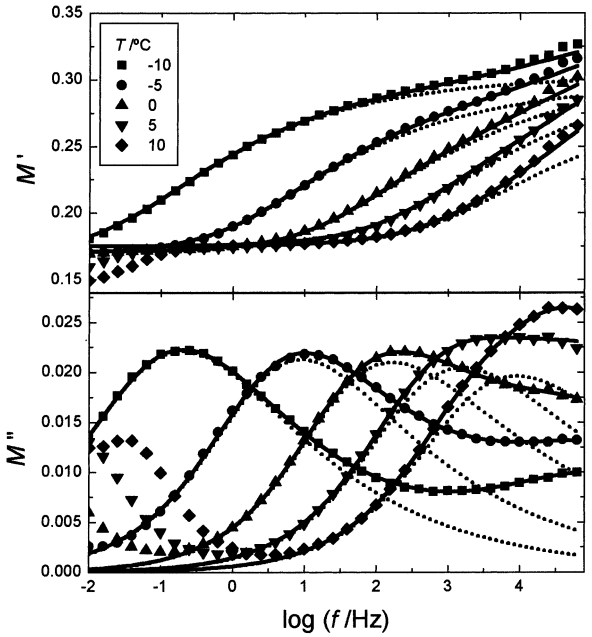


**Figure 5.** Real and imaginary components of the dielectric modulus in the α-relaxation region. The solid lines correspond to the fit with the sum of two HN functions. The dotted lines discriminate the low-frequency process of the fitting (α-relaxation).

tation of the original HN function for complex permittivity, $\epsilon^*(\omega)$:[39]

$$M^*(\omega) = M_U + \frac{M_R - M_U}{[1 + (i\omega\tau_{HN})^a]^b} \quad (5)$$

where $\tau_{HN}$ is the central relaxation time, and, again, U and R designate unrelaxed (i.e., $\tau_{HN}\omega \rightarrow \infty$) and relaxed (i.e., $\tau_{HN}\omega \rightarrow 0$) moduli values of the single process. $a$ and $b$ are shape parameters ($0 < a \leq 1$ and $0 < b \leq 1$) which correspond to symmetric and asymmetric broadening of the distribution of relaxation times, respectively. The fitting curves (solid lines in Figure 5) agree well with the experimental data for both moduli components. The dotted lines correspond to the α-relaxation component of the fitting. Values of $a$ between 0.5 and 0.6 and values of $b$ between 0.3 and 0.5 were obtained for this process at the different temperatures. Such values are in accordance to those found for the dielectric or mechanical α-process in simple polymers. The relaxation time at each temperature, $\tau$, associated with the maximum loss can be related to $\tau_{HN}$ by[36]

$$\frac{\tau_{HN}}{\tau} = \left[\sin\left(\frac{\pi a}{2}\right)/\tan\left(\frac{\pi a}{2(b+1)}\right) - \cos\left(\frac{\pi a}{2}\right)\right]^{-1/a} \quad (6)$$

The Arrhenius diagrams for the mechanical and dielectric α-relaxation of LCP1 are shown in Figure 6, with $\tau = 1/(2\pi f_{max})$ being $f_{max}$ the frequency of maximum loss. The open squares correspond to the relaxation times, obtained from the $\tau_{HN}$ values resulting from the fittings according to eq 5 and then transformed to $\tau$ with eq 6. The open circles correspond to the relaxation times that were obtained by looking at the maximum of loss permittivity, $\epsilon''$, from the data reported in ref 37. The solid squares correspond to mechanical spectroscopic results adapted from the obtained shift factors (inset graphics in Figure 3). In fact, from log $a_T$ = log $\tau(T)/\tau(T_{ref})$ we have log $\tau(T)$ = log $a_T$ + log $\tau(T_{ref})$.

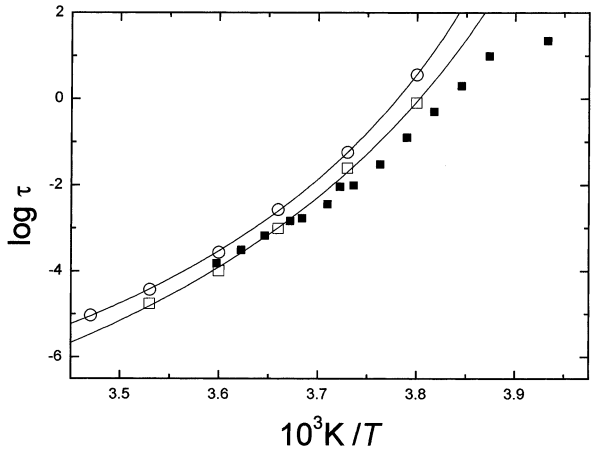


**Figure 6.** Arrhenius plot including dielectric (open symbols) and mechanical (solid squares) results for the α-relaxation of LCP1. The open squares are for the dielectric relaxation times obtained from the analysis of the $M''$ curves. The open circles are for the dielectric retardation times, obtained from the analysis of the $\epsilon''$ curves. Both point sets were fitted with the VFT equation (solid lines). The mechanical relaxation times were obtained from the analysis of the data in Figure 4.

As log $\tau(T_{ref} = -3.6\ °C) = -2.45$, obtained from the KWW fitting, it is easy to construct the Arrhenius log $\tau$ vs $1/T$ plot from the log $a_T$ data.

Figure 6 shows that the mechanical and dielectric retardation times (squares) satisfactorily agree at higher temperatures. With decreasing temperature the dielectric relaxation times tends to increase more rapidly than the mechanical ones. The differences observed between the mechanical and dielectric results can be attributed to the different molecular effects imposed and measured during the use of the two experimental techniques. However, the Arrhenius diagram strongly suggests that the molecular attribution of the α-relaxation obtained from both methods is formally the same. Moreover, similar values of $\beta_{KWW}$ obtained from calorimetric, mechanical, and dielectric experiments, as well as the location of the α-relaxation at low frequencies in the vicinity of the glass transition temperature, also strengthen for the common origin of the process observed by the different techniques, which should be assigned to the cooperative segmental motions of the polymer backbone. However, the two possibilities discussed in section II could be directly linked. In fact, inside the so-called cooperative rearranging regions (CRR), which comes from the Adam−Gibbs theory, one should have a number of mesogens, besides the atoms from both polymer backbones and spacers. A CRR is defined as a region that contains a number of molecular groups that can undergo a conformational transition without disturbing the neighboring groups. Therefore, in SCLCPs, any conformation change within the polymer backbone, associated with the glass transition event, should involve obligatorily motions within the mesogenic groups, which are intimately correlated to the segmental motions in the polymer chain. This will happen even in the smectic phase where mesogenic groups may undergo rotational/translational at least within the layer where they are located. The onset of the mobility of these stiff and bulky mesogenic groups will be then decisive in the occurrence of the glass transition. Note, in this context, that the glass transition temperature of the linear poly(dimethylsiloxane) corresponding to the backbone of LCP1 is −124 °C,[40] i.e.,

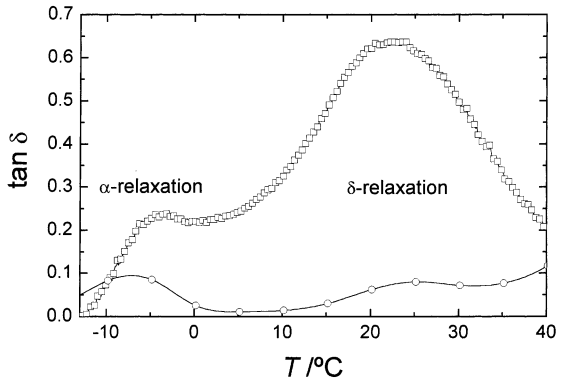


**Figure 7.** Temperature dependence of the loss factor (1 Hz) from compression mechanical spectroscopy results (squares) and from dielectric data (circles) in the region of the α- and δ-relaxations.

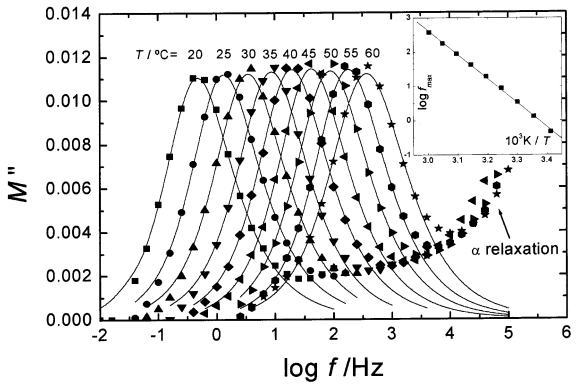


**Figure 8.** Dielectric loss modulus in the δ-relaxation region. The solid lines correspond to the fit with one HN function. The frequency at maximum $M''$ is plotted against reciprocal temperature in the inset Arrhenius diagram, where the Arrhenius fit was included.

almost 120 K below the $T_g$ of LCP1, indicating the hindering effect of the mesogenic groups. In dielectric spectroscopy the measured response is essentially probed by the motions in the mesogenic groups, due to the low polarity of the backbone. Additionally, the first degrees of freedom that are dielectrically liberated in these groups are probably associated with the 10, 01, and 11 modes, discussed in section II. In fact, as commented by Attard based on previous theories,[41] these modes have similar relaxation times, while the 00 mode, which would be related to the occurrence of the δ-relaxation, has higher characteristic times; thus, the δ-relaxation is expected to appear at higher temperatures for the same experimental frequency. The fastest motions involving mainly $\mu_t$ can be sufficient ample to permit the occurrence of the glass transition. Therefore, the onset of the glass transition, as seen directly by calorimetric or mechanical spectroscopy techniques, can be intimately connected to release of the fastest motions in the mesogenic groups, measured by dielectric spectroscopy.

The dielectric data depicted in Figure 5 display a clear non-Arrhenius behavior which can be well parametrized with the VFT expression

$$\tau = \tau_0 \exp\left(\frac{DT_0}{T - T_0}\right) \tag{7}$$

where $\tau_0$ is the reciprocal of an attempt frequency, $T_0$ is the temperature where the characteristic times seems to diverge, and $D$ is the strength parameter which is related to the fragility concept first introduced by Angell.[42] From the $M''$ data (open squares in Figure 6) the fitting of the temperature dependence of the relaxation times yield $\tau_0 = 2.47 \times 10^{-13}$ s, $T_0 = -43.1$ °C, and $D = 4.15$. From the $\epsilon''$ data (circles in Figure 6) the fitting of the temperature dependence of the retardation times yield $\tau_0 = 8.75 \times 10^{-12}$ s, $T_0 = -36.8$ °C, and $D = 3.0$. Despite the different values for the fitting parameters the two Vogel−Fulcher lines in Figure 6 are quite parallel; i.e., both characteristic times exhibit similar changes with temperature. This can be explained by some statistical compensation effects between the VFT parameters; i.e, different sets of $T_0$ and $D$ can lead to VFT plots with similar curvature. The same parallelism between relaxation and retardation times when plotted against temperature was observed by other authors.[43]

**C. Rheological and Dielectric Results in the Region of the δ-Relaxation.** *1. General Features of the δ-Relaxation.* The viscoelastic response above $T_g$, i.e., in the smectic region, was accessed by compression DMA experiments. The temperature dependence of the obtained loss factor at 1 Hz is shown in Figure 7. A broad relaxation process is observed above the α-relaxation temperature region, between 5 and 40 °C. For a better comparison the dielectric loss factor at 1 Hz is also depicted in the same graphics, extracted from isothermal experiments.[37] The dielectric δ-relaxation, with a maximum of tan δ at ∼25 °C, seems to correlate well with the mechanical peak with respect to the location in the temperature axis. Simon et al. also detected a mechanically active relaxation, as a shoulder just above the glass transition relaxation peak.[11] This relaxation was assigned to thermal disruption of the weak "cross-linking" effect of the liquid crystalline domains, which leads to the freeing of side-chain mesogenic motions.[11] This attributions is consistent with the general assignment of the δ-relaxation.

For further comparisons between the mechanical and dielectric experiments a deeper analysis of this process was carried out. Again, the dielectric data of the δ-process reported in ref 37 were rebuilt in terms of $M^*$. The dielectric loss modulus in this temperature region is shown in Figure 8.

The solid lines in Figure 8 are the fittings of the data according to the HN model (eq 5). The high-frequency points were ignored because they are greatly influenced by the α-relaxation. It was found that both $a$ and $b$ parameters do not depend strongly on temperature, at least in the smectic phase, where the results were analyzed. The average values of the HN parameters through the nine temperatures gave $a = 0.94 \pm 0.03$ and $b = 0.76 \pm 0.04$. From this result one can conclude that the δ-relaxation is characterized by a very small symmetric broadening about the central relaxation time $\tau_{HN}$, i.e., a narrow distribution of relaxation times, because $a$ is close to 1. Moreover, since $b$ is also high, the existing distribution has also low asymmetry. This is very consistent with the attribution of the δ-relaxation to a quasi-Debye process that is often found in the literature on other SCLCPs systems.[23,24,26,30]

The fitting of the data in Figure 8 also allowed to obtain the temperature dependence of $\tau_{HN}$ that, after being transformed according to eq 6, can be used to build an Arrhenius plot (inset graphics in Figure 8). This plot shows a weak curvature and was fitted with the Arrhenius equation, $\log f_{max} = \log f_0 - E_a/[RT \ln(10)]$.

The obtained activation energy in this temperature region was $E_a = 134$ kJ mol$^{-1}$ and $\tau_0 = 1/(2\pi f_0) = 2.71 \times 10^{-25}$ s. It should be noted that the Arrhenius plot of LCP1 displays a change in slope when the temperatures pass above the clearing temperature, above which the apparent activation energy decreases.[37] The same behavior was also found on the $\delta$-relaxation of on nematic and smectic LCPs.[6,21,44−46] In that study the activation energy for the loss permittivity data in a broad temperature range was 159.2 kJ mol$^{-1}$ in the smectic phase and 110.5 kJ mol$^{-1}$ in the isotropic phase. This difference is the result of the less constrained mobility of the mesogenic moieties in the isotropic liquid state. Other authors also point out for the Arrhenius behavior of the $\delta$-relaxation.[46−49] Moreover, the apparent activation energies of the $\delta$-relaxation observed in other nematic or smectic SCLCPs are found to range between 120 and 180 kJ mol$^{-1}$,[6] strengthening the attribution of the $\delta$-relaxation of LCP1 to the same mechanism. There are also some works were a curvature is clearly observed, and the VFT model is proposed to describe the dynamics of the $\delta$-process.[23,26] The Arrhenius or VFT nature of the $\delta$-relaxation is thus an open problem, and other studies should be carried out in order to elucidate it without ambiguity. Nevertheless, one should expect that the assigned motions should slow down and even freeze near $T_g$, and thus an Arrhenius behavior in the lower temperature region of the liquid crystalline phase cannot be expected as it predicts finite mobility in the glassy state.

For a better comparison between the mechanical and dielectric results an attempt to simulate the mechanical loss modulus was carried out with the dielectric data. Simple assumptions, supported by experimental evidence, were made, namely: a HN description of the data with temperature-independent $a$ and $b$ parameters; a simple Arrhenius dependence for the relaxation times, $\tau(T)$, described by the fitting parameters obtained from the dielectric results; and a constant mechanical strength $E'_R - E'_U$ that was estimated from the mechanical data as being ≈180 MPa for the $\delta$-relaxation. The expression used for computing $E''$ corresponds to the imaginary component of eq 5 for the mechanical complex modulus, written in the temperature domain, and was adapted from the dielectric formalism:[50]

$$E''(T) = \frac{(E_R - E_U)\sin[b\varphi(T)]}{\left\{1 + 2[\omega\tau(T)]^a \sin\left[\frac{1}{2}\pi(1-a)\right] + [\omega\tau(T)]^{2a}\right\}^{b/2}} \quad (8)$$

where

$$\varphi(T) = \text{arctg}\frac{[\omega\tau(T)]^a \cos\left[\frac{1}{2}\pi(1-a)\right]}{1 + [\omega\tau(T)]^a \sin\left[\frac{1}{2}\pi(1-a)\right]} \quad (8)$$

and, in this case, $\omega = 2\pi f = 6.283$ s$^{-1}$.

The simulation of the mechanical behavior using dielectric data and eq 8 is shown in Figure 9 (solid lines). It can be compared with the experimental mechanical loss response (squares). Taking into account the strong influence of the α-relaxation, which appears in the low-temperature side, we may conclude that the higher temperature region of the experimental $E''$ results is well described by the prediction using parameters obtained from dielectric data. This result strength the idea that a similar origin for the dielectric process should be attributed to the mechanical one.

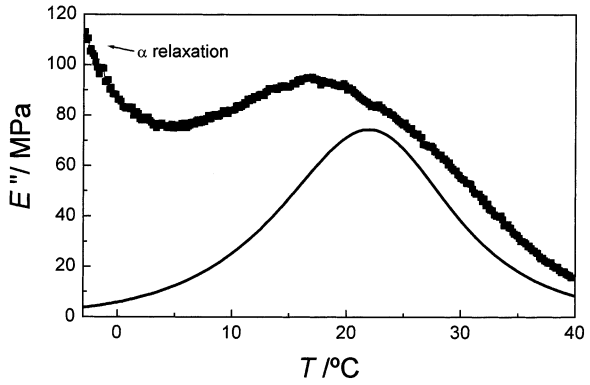


**Figure 9.** Squares: mechanical loss modulus at 1 Hz in the region of the $\delta$-relaxation. Solid line: simulation of the process using dielectric data, which was used to describe the distribution of relaxation times and the temperature dependence of the mean relaxation time (see text).

As said before, the dielectric $\delta$-relaxation should be assigned to the motions within the mesogenic groups, activated by the longitudinal component of the dipolar moment. As refereed by Attard, Williams, and coworkers,[46] it is not expected that the dipoles reverse completely, as it happens in low molecular weight liquid crystals, due to the topological constraints of the polymer system. A hypothesis suggested by these authors is that the mesogens undergo fluctuations within a cone. In the smectic phase, it is possible that the mesogens also jump from one to another layer. The occurrence of the $\delta$-relaxation, probed by dielectric experiments, is then associated with the onset of a much more facilitated conformational mobility of the mesogens. This leads to an expected change upon the relevant rheological properties, e.g., mechanical modulus or compliance, in the same temperature/time scale region with the corresponding rise of a mechanical relaxation process.

*2. Comparison with DSC Results.* It is interesting to notice that no change is detected in the heat flux in the DSC result in the temperature range of the $\delta$-relaxation (Figure 1). A jump in the heat capacity analogous to a glass transition implies a change in the temperature dependence of the number of microstates Ω available for the polymer chains (as deduced form the Boltzmann's formula $S = k \ln \Omega$ and $C_p = T\,\mathrm{d}S/\mathrm{d}T = kT\,\mathrm{d}\ln\Omega/\mathrm{d}T$). This is the case in the glass transition because of the exponential increase of the number of configurational states with increasing temperature in the liquid state. In the $\delta$-relaxation the gain of molecular freedom during the occurrence of this process is done by motions of stiff groups as a whole. Such motions does not involve significant variations in the number of microstates with temperature, given by the Ω parameter, that quantifies the number of possible conformational rearrangements of the activated state that lead to the same prescribed macroscopic properties. Therefore, the heat capacity is not expected to experiment a considerable increase throughout the development of the $\delta$-relaxation. The same invariance of Ω also happens with the secondary relaxations and also relaxation processes taking place at temperatures above the glass transition as the so-called $\alpha_c$ relaxation. This process is observed in flexible semicrystalline polymers, being attributed to the occur-

rence of screwlike motions within the crystalline lamellae (refs 51−53 and references cited therein). Thus, also in that case the increase of Ω with temperature is not extensive, and thus it is not observed by DSC.

The $\alpha_c$-process also exhibits a near-Debye dielectric response, as found in the $\delta$-relaxation in SCLCPs. Another example of near-Debye behavior is the relaxation process associated with the interfacial polarization or Maxwell−Wagner process that also takes place at temperatures higher than the glass transition.

On the contrary, secondary processes show usually a broad distribution of relaxation times, which can be related to the fact that the neighborhood of the relaxing species is not homogeneous (although there is the alternative explanation given by the coupling mode mentioned above). The potential energy barrier hindering the motion of the relaxing groups is created by parts of the polymer chains that have relaxation times which are much higher than that of the relaxing species and thus are nearly static. A relatively narrow distribution of activation energies can cause a broad distribution of relaxation times. Also, the main dynamic-mechanical or dielectric relaxation associated with the cooperative rearrangements of the main-chain segments shows broad relaxation times spectra. In this process the energy barriers hindering the motion are created by molecular groups which have the same dynamics and are distributed inhomogeneously (due to the inhomogeneity of the free volume distribution along the material) around the polymer segment that suffers a conformational rearrangement. In the case of the relaxation that takes place in the liquid state, the relaxation time of any group in the polymer chain, including the cooperative rearrangements of the main chains of the polymer, is much smaller than the one of the relaxing groups. If the cooperativity of the relaxation process is not high, the dynamics of the relaxing species tends to be very homogeneous, as the motion of the group in a viscous media. This can explain that many relaxation processes that occurs at temperatures above the glass transition present narrow distributions of relaxation times.

## V. Conclusions

The relaxation processes occurring in the glassy state of SCLCPs are local and thermally activated and have been often reported in the literature, mainly dielectric spectroscopy studies. On the other hand, the liquid crystalline state (near the clearing temperature) and the isotropic liquid phase have been well characterized from rheological studies. In this work, the molecular mobility in a SCLCP was investigated in the temperature region comprising the glass transition and the smectic phase. The two main relaxation processes that generally appear in such systems have been scarcely studied by mechanical spectroscopy methods, although dielectric spectroscopy has been widely used.

The origin of the α-relaxation at the molecular level has been controversial. It was shown in this work that the mechanical α-process has many similarities with the dielectric one and with the calorimetric glass transition, being assigned to the dynamic glass transition of the polymer. The dielectric process could be assigned to the onset of special modes within the mesogens, but such motions are intimately correlated with the dynamics of the polymer backbone. Therefore, the discrimination between both kind of motions is complex using such techniques.

The $\delta$-relaxation of the studied material starts to occur at ambient temperature, just above the glass transition, as it happens for a great number of other SCLCPs. Thus, the viscoelastic properties of such materials highly depend on this process. It was demonstrated that the mechanical and dielectric $\delta$-relaxation is formally the same. The $\delta$-relaxation should involve mainly the motions of the bulky mesogens, being the reason why this process is not observable by calorimetric methods. Such motions could be a result of fluctuations in the redistribution of the orientatinal distribution function of the mesogenic groups, mainly along the longitudinal component of the dipolar moment.

**Acknowledgment.** The assistance of Prof. Madalena Dionísio (Univ. Nova de Lisboa) in the data treatment is acknowledged.

## References and Notes

(1) *Side Chain Liquid Crystal Polymers*; McArdle, C. B., Ed.; Blackie and Son Ltd.: Glasgow, 1989.
(2) *Liquid Crystalline and Mesomorphic Polymers*; Shibaev, V. P., Lam L., Eds.; Springer-Verlag: Berlin, 1994.
(3) Ediger, M. D.; Angell, C. A.; Nagel, S. R. *J. Phys. Chem.* **1996**, *31*, 13200−13212.
(4) Angell, C. A.; Ngai, K. L.; McKenna, G. B.; McMillan, P. F.; Martin, S. W. *J. Appl. Phys.* **2000**, *88*, 3113−3157.
(5) Ngai, K. L.; Etienne, S.; Zhong, Z. Z.; Schuele, D. E. *Macromolecules* **1995**, *28*, 6423−6431.
(6) Simon, G. P. In *Dielectric Spectroscopy for Polymers*; Runt, J., Fitzgerald, J., Eds.; American Chemical Society: Washington, DC, 1997.
(7) Kannan, R. M.; Kornfield, J. A.; Schwenk, N.; Boeffeld, C. *Macromolecules* **1993**, *26*, 2050−2056.
(8) Rubin, S. F.; Kannan, R. M.; Kornfield, J. A.; Boeffel, C. *Macromolecules* **1995**, *28*, 3521−3530.
(9) Wewerka, A.; Viertler, K.; Vlassopoulos, D.; Stelzer, F. *Rheol. Acta* **2001**, *40*, 416−425.
(10) Wewerka, A.; Floudas, G.; Pakula, T.; Stelzer, F. *Macromolecules* **2001**, *34*, 8129−8137.
(11) Simon, G. P.; Kozak, A.; Williams, G.; Wetton, R. E. *Mater. Forum* **1991**, *15*, 71−81.
(12) Etienne, S.; David, L.; Mitov, M.; Sixou, P.; Ngai, K. L. *Macromolecules* **1995**, *28*, 5758−5764.
(13) Zentel, R.; Strobl, G. R.; Ringsdorf, H. *Macromolecules* **1985**, *18*, 960−965.
(14) Vallerien, S. U.; Kremer, F.; Boeffel, C. *Liq. Cryst.* **1989**, *4*, 79−86.
(15) Romero Colomer, F.; Meseguer Dueñas, J. M.; Gómez Ribelles, J. L.; Barrales Rienda, J. M.; Bautista Ojeda, J. M. *Macromolecules* **1993**, *26*, 155−166.
(16) Gedde, U. W.; Liu, F.; Hult, A.; Sahlén, F.; Boyd, R. H. *Polymer* **1994**, *35*, 2056−2062.
(17) Williams, G. *Polymer* **1994**, *35*, 1915−1922.
(18) Andrews, S. R.; Williams, G.; Läsker, L.; Stumpe, J. *Macromolecules* **1995**, *28*, 8463−8469.
(19) Attard, G. S.; Araki, K.; Williams, G. *Br. Polym. J.* **1987**, *18*, 119−127.
(20) Haase, W.; Pranoto, H.; Bormuth, F. J. *Ber. Bunsen-Ges. Phys. Chem.* **1985**, *89*, 1229−1234.
(21) Seiberle, H.; Stille, W.; Strobl, G. *Macromolecules* **1990**, *23*, 2008−2016.
(22) Zhong, Z. Z.; Schuele, D. E.; Smith, S. W.; Gordon, W. L. *Macromolecules* **1993**, *26*, 6403−6409.
(23) Zhong, Z. Z.; Gordon, W. L.; Schuele, D. E.; Akins, R. B.; Percec, V. *Mol. Cryst. Liq. Cryst.* **1994**, *238*, 129−145.
(24) Zhong, Z. Z.; Schuele, D. E.; Gordon, W. L. *Liq. Cryst.* **1994**, *17*, 199−209.
(25) Kim, H. J.; Jackson, W. R.; Simon, G. P. *Eur. Polym. J.* **1994**, *30*, 1201−1207.
(26) Mijovic, J.; Sy, J. W. *Macromolecules* **2000**, *33*, 9620−9629.
(27) Kremer, F.; Vallerien, S. U.; Zentel, R.; Kapitza, H. *Macromolecules* **1989**, *22*, 4040−4045.
(28) Schönhals, A.; Wolff, D.; Springer, J. *Macromolecules* **1998**, *31*, 9019−9025.
(29) Mano, J. F.; Alves, N. M.; Meseguer Dueñas, J. M.; Gómez Ribelles, J. L. *Polymer* **1999**, *40*, 6545−6556.

(30) Schick, C.; Sukhorukov, D.; Schönhals, A. *Macromol. Chem. Phys.* **2001**, *202*, 1398−1404.
(31) Ferry, J. D. *Viscoelastic Properties of Polymers*, 3rd ed.; John Wiley & Sons: New York, 1980.
(32) Alegria, A.; Echevarría, E. G.; Goitiandía, L.; Tellería, I.; Colmenero, J. *Macromolecules* **1995**, *28*, 1516−1527.
(33) Williams, G. In *Structure and Properties of Polymers* in *Dielectric Properties of Polymers in Materials Science and Technology Series*; Thomas, E., Ed.; VCH Publishers: London, 1993; Vol. XII, p 471.
(34) Kohlrausch, F. *Poggendorff's Ann. Phys.* **1863**, *119*, 352.
(35) Williams, G.; Watts, D. C. *Trans. Faraday Soc.* **1970**, *66*, 80.
(36) Schröter, K.; Unger, R.; Reissig, S.; Garwe, F.; Kahle, S.; Beiner, M.; Donth, E. *Macromolecules* **1998**, *31*, 8966−8972.
(37) Mano, J. F.; Correia, N. T.; Moura Ramos, J. J.; Andrews, S. R.; Williams, G. *Liq. Cryst.* **1996**, *20*, 201−217.
(38) Gómez, D.; Alegria, A.; Arbe, A.; Colmenero, J. *Macromolecules* **2001**, *34*, 503−513.
(39) Havriliak, S.; Negami, S. *J. Polym. Sci., Part C* **1966**, *14*, 99.
(40) Kirst, K. U.; Kremer, F.; Pakula, T.; Hollingshurst, J. *Colloid Polym. Sci.* **1994**, *272*, 1420−1429.
(41) Attard, G. S. *Mol. Phys.* **1986**, *58*, 1087−1100.
(42) Angell, C. A. *J. Non-Cryst. Solids* **1991**, *131*−*133*, 13−31.
(43) Meseguer Dueñas, J. M.; Vidaurre Garayo, A.; Romero Colomer, F.; Más Estellés, J.; Gómez Ribelles, J. L.; Monleón Pradas, M. *J. Polym. Sci., Polym. Ed.* **1997**, *35*, 2201−2217.
(44) Kresse, H.; Talrose, R. V. *Makromol. Chem., Rapid Commun.* **1981**, *2*, 369−374.
(45) Kresse, H.; Kostromin, S.; Shibaev, V. P. *Makromol. Chem., Rapid Commun.* **1982**, *3*, 509−513.
(46) Attard, G. S.; Williams, G.; Gray, G. W.; Lacey, D.; Gammel, P. A. *Polymer* **1986**, *27*, 185−189.
(47) Böhme, A.; Novotna, E.; Kresse, H.; Kuschel, F.; Lindau, J. *Makromol. Chem.* **1993**, *194*, 3341−3348.
(48) Day, G. M.; Jackson, W. R.; Simon, G. P. *Eur. Polym. J.* **1998**, *34*, 439−444.
(49) Akiyama, E.; Nagase, Y.; Koide, N.; Araki, K. *Phys. Chem. Chem. Phys.* **1999**, *1*, 2319−2326.
(50) Böttcher, C. J. F.; Bordewijk, P. *Theory of Electric Polarization*, 2nd ed.; Elsevier: Amsterdam, 1978; Vol. II.
(51) Boyd, R. H. *Polymer* **1985**, *26*, 323−347.
(52) Mano, J. F.; Sousa, R. A.; Reis, R. L.; Cunha, A. M.; Bevis, M. J. *Polymer* **2001**, *42*, 6187−6198.
(53) Mano, J. F. *Macromolecules* **2001**, *34*, 8825−8828.

MA020800P